Numerical investigation of anti-sloshing performance of hanging porous part in rectangular tank

Chenyi Wang[a], Changfang Zou[a,b*], Xiaonan Yuan[a], Sheng Ding[c], Quanming Miao[a]
[a] School of Ocean Engineering, Jiangsu Ocean University, Lianyungang 222000, China; [b] Jiangsu Institute of Marine Resources Development, Lianyungang 222000, China; [c] Ciel&Terre (Shanghai) New Energy Technology Co., Ltd., Shanghai 200000, China

ABSTRACT

As a non-negligible problem, the suppression of sloshing is very important for liquid storage carriers such as LNG (Liquefied Natural Gas) ships. The effective suppression of impact pressure caused by sloshing liquid improves the safety of the structure. In this paper, the porosity characteristic is combined with the adjustable hanging part, and the effects of this composite anti-sloshing method on sloshing states are studied by CFD (Computational Fluid Dynamics). The results show that, compared with the traditional solid part, the composite method with appropriate porosity can further suppress the sloshing, and the load acting on the hanging porous part induced by the sloshing liquid is smaller. When the porous part near the static free surface moves downward, the damping effect enhances, leading to further improvement of the anti-sloshing effect, but the load acting on the part increases.

Keywords: Suppressing sloshing, impact pressure, composite method, damping effect, numerical simulation

1. INTRODUCTION

Sloshing, as one of the top research problems in the field of fluid mechanics, is widely found in all types of transport equipment with partial filling liquid. In liquid storage carriers with free liquid surface, the liquid sloshing caused by external excitation will affect the movement of the carrier and the safety of the structure. In the field of marine construction, the effect of sloshing is an important factor that cannot be ignored in the design of storage carriers such as LNG ships. The liquid in the tank may move violently when the filling level of the LNG ship is between 10%-70%. Especially in the low filling level of about 30%, the sloshing liquid will have a great impact on the structure[1]. Where the frequency of the external excitation approximates the natural frequency of the liquid in the tank, the strong impact will threaten the safety of the structure or even destroy the local structure[2].

The anti-sloshing methods can be mainly divided into active suppressing and passive suppressing. The active anti-sloshing methods require external control to interfere in the movement of free liquid. Hara and Shibata proposed a method of injecting bubbles into the liquid in the cabin to suppress sloshing and studied injection timing and injection volume to obtain an algorithm to control the injection time and duration[3]. Zou et al. also numerically investigated the effect of compressible air and the liquid of different viscosities on the sloshing state[4]. Hernandez and Santamarina studied the active vibration control method by FEM and verified the effectiveness of this method through experiments[5]. The passive anti-sloshing methods mainly include fixed structures and floating structures. Shao et al. numerically studied the anti-sloshing effect of fixed baffles with different shapes and locations by the SPH method. They found that the T-shaped baffle has a great anti-sloshing effect, and the reason is that it had more tips to reduce the kinetic energy of the sloshing liquid[6]. The energy dissipation due to viscous friction has also been demonstrated can effectively suppress sloshing pressure by Zou et al.[7]. Ünal et al. used the finite difference and finite volume methods to investigate the effect of the height ratio of the T-baffle to the static free surface on the sloshing pressure and wave elevation. The results show that the T-shaped baffle can suppress sloshing more effectively when its height is beyond 80% of the static free surface. They considered that the suppression effect of the T-shaped baffle is related to wall shear, blockage effect and energy dissipation due to vortexes[8]. In terms of the floating structure, Koh et al. designed a novel floating device, which takes the rectangular box as the main body, and the bottom of the box is connected with the centre of the bilge through four cables. The numerical simulation and experiment show that this method has a good anti-sloshing effect[9]. Yu et al. presented a movable baffle that could

* zchf1983@aliyun.com

Third International Conference on Computer Science and Communication Technology (ICCSCT 2022)
edited by Yingfa Lu, Changbo Cheng, Proc. of SPIE Vol. 12506, 125062G
 · 0277-786X · doi: 10.1117/12.2661851

always float on the free surface, and it can only move in the vertical direction through the slide. They numerically and experimentally proved that this floating device has a good anti-sloshing effect[10].

In recent years, porous materials have attracted more and more attention because they can consume the energy of sloshing liquid effectively. Zang et al. designed a horizontal ring porous baffle and analysed its optimal porosity, angle and height through numerical calculation[11]. The porous media is also been employed to attach to the inner wall of the liquid tank to suppress sloshing by Xue et al.. They numerically studied the anti-sloshing effect of the porous media layer under extreme sloshing conditions[12]. Based on these studies, it can be seen that porous media plays a certain role in suppressing sloshing, which has a broad application prospect.

In view of a good anti-sloshing effect of the vertical parts directly acting on the free surface and the advantages of the porous parts in reducing liquid kinetic energy, the anti-sloshing performance of a light net porous vertical part set in middle of the tank along the length is numerically studied by CFD in this paper. This method combines the characteristics of vertical parts with porous parts. The part only keeps the movement in the vertical direction, and it always keeps a certain distance from its horizontal midline to the static free surface. The effects of porosity and midline offset on the anti-sloshing performance are also studied for a more comprehensive understanding of this method.

2. NUMERICAL METHOD

2.1 Governing equations

For sloshing in tank, the internal fluid satisfies the continuity equation and the RANS equation. The equations are shown below:

(1) Continuity equation:

$$\frac{\partial \rho}{\partial t}+\frac{\partial}{\partial x_i}\left(\rho u_i\right)=0 \tag{1}$$

(2) RANS equation:

$$\rho \frac{\partial \overline{u_i}}{\partial t}+\rho \overline{u_j} \frac{\partial \overline{u_i}}{\partial x_j}=\rho \overline{F_i}-\frac{\partial \overline{p}}{\partial x_i}+\frac{\partial}{\partial x_j}\left(\mu \frac{\partial \overline{u_i}}{\partial x_j}-\rho \overline{u_i' u_j'}\right) \tag{2}$$

where u_i is the velocity in i direction, $\overline{u_i}$ is the average velocity and u_i' is the fluctuating velocity. $\overline{p}$ is the total pressure on the element and $\overline{F_i}$ is the mass force on the fluid element, μ is the dynamic viscosity and ρ is the density. Sloshing approaching resonance is a classical turbulence problem, and the numerical simulations based on CFD are generally performed using the k-ε, the k-ω SST or the LES models. The standard k-ε model is employed in this paper and its transport equations are shown below:

$$\frac{\partial}{\partial t}(\rho k)+\frac{\partial}{\partial x_i}(\rho k u_i)=\frac{\partial}{\partial x_i}\left(\left(\mu+\frac{\mu_t}{\sigma_k}\right)\frac{\partial k}{\partial x_j}\right)+G_k+G_b-\rho\varepsilon-Y_M+S_k \tag{3}$$

$$\frac{\partial}{\partial t}(\rho \varepsilon)+\frac{\partial}{\partial x_i}(\rho \varepsilon u_i)=\frac{\partial}{\partial x_j}\left(\left(\mu+\frac{\mu_t}{\sigma_\varepsilon}\right)\frac{\partial \varepsilon}{\partial x_j}\right)+C_{1\varepsilon}\frac{\varepsilon}{k}\left(G_k+C_{3\varepsilon}G_b\right)-C_{2\varepsilon}\rho\frac{\varepsilon^2}{k}+S_\varepsilon \tag{4}$$

where G_k and G_b are the derived terms of turbulent kinetic energy k, G_k is due to the average velocity gradient, G_b is due to the buoyancy and μ_t is the turbulent viscosity. $C_{1\varepsilon}$, $C_{2\varepsilon}$, $C_{3\varepsilon}$, σ_k, σ_ε are the empirical constant and can be 1.44, 1.92, 0.09, 1.0, and 1.3 respectively in this research.

Under the action of pores, the momentum loss of sloshing fluid flowing through the porous parts satisfies Darcy's law. The inertia loss of the sloshing fluid cannot be ignored under the conditions of high Reynolds number[13]. Therefore, Darcy's law with inertia loss correction should be considered to characterize the resistance source term. The resistance source term of the fluid momentum is shown as follows:

$$S = -\frac{\mu}{a}v + \left(-C_u \cdot \frac{1}{2}\rho |v| v \right) \tag{5}$$

where a is the permeability, C_u is the inertial resistance factor and v is the velocity of the liquid. a and C_u can be determined by the Ergun formula:

$$a = \frac{D_P{}^2}{150} \cdot \frac{\varphi^3}{\left(1-\varphi^2\right)} \tag{6}$$

$$C_u = \frac{3.5}{D_P} \cdot \frac{1-\varphi}{\varphi^3} \tag{7}$$

where D_p is the mean particle diameter and φ is the porosity.

2.2 Free surface tracking: VOF method

When the frequency of external excitation approaches the natural frequency of the sloshing liquid, the free surface shows the complicated flow, such as breaking and wrapping bubbles. The VOF method, an effective technique for capturing highly non-linear free surface, is employed in this research to accurately treat the free surface of sloshing liquid. It is assumed that all liquids in the tank are incompressible, the VOF method is shown below:

$$\frac{\partial \alpha_w}{\partial t} + \mathbf{U} \cdot \nabla \alpha_w = 0 \tag{8}$$

$$\alpha_w + \alpha_a = 1 \tag{9}$$

where $\mathbf{U}$ is the velocity field, α_w is the volume fraction of water and α_a is the volume fraction of air. $\alpha_w = 1$ means that all the units are water and $0 < \alpha_w < 1$ means that the units contain both water and air. When there are two phases contained in the unit, the equivalent density ρ' and equivalent viscosity μ' can be obtained by the formulas below:

$$\rho' = \alpha_w \rho_w + (1-\alpha_w)\rho_a \tag{10}$$

$$\mu' = \alpha_w \mu_w + (1-\alpha_w)\mu_a \tag{11}$$

where the subscript w is for the parameters of water and the subscript a is for the parameters of air. Assuming no slip and no mass exchange between the two-phase interface of air and water, and the velocity field is continuous. The equivalent density ρ' and equivalent viscosity μ' will be applied to the continuity equation and the RANS equation.

3. COMPUTATIONAL MODEL

3.1 Model tank and excitation

As the cross sections of the rectangular tank along its length are the same size everywhere, and differences between the 3D and the 2D models where is away from the corners are negligible [14]. The 3D model of the tank can be simplified to the 2D model in this research.

Figure 1 shows the cross section of the model tank. The model tank has a rectangular shape with dimensions (B×H) of 0.97 m×0.927 m, which is of the same section size as the model tank used in the experiment of Wei et al. (2015)[15]. h_w is the height of the static free surface an h_b is the height of the porous part which is 0.1854m (20%H). The midline offset λ is the distance between the midline of the part and the static free surface, $\lambda > 0$ means the midline is above the static free surface. The porous media model is applied to study the effects of the hanging porous part on sloshing in this research, without considering the deformation of the wall and porous part.

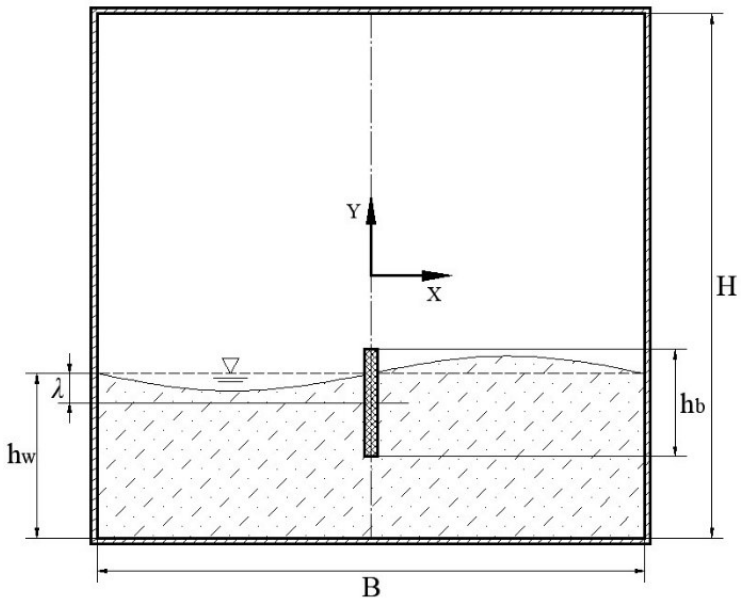

Figure 1. Illustration of the model tank and the hanging porous part.

The tank sways in the single-degree-of-freedom in the width direction. The horizontal harmonic excitation of the displacement is as follows:

$$x = A\sin(2\pi ft) \tag{12}$$

where A is the excitation amplitude and t is time. f is the excitation frequency and the natural frequencies of sloshing liquid in the tank are selected as the excitation frequencies in this research. The natural frequency f_0 can be estimated by the formula given by Liu and Lin (2008)[16]:

$$f_0 = \frac{1}{2\pi}\sqrt{\frac{n\mathrm{g}\pi}{\mathrm{B}}\tanh(\frac{n\pi}{\mathrm{B}}\mathrm{h_w})}, n = 1,2,3\ldots \tag{13}$$

The sloshing liquid in the tank is water, and the initial pressure of the air above the water is 101325 Pa. Gravitational acceleration g is 9.8m/s^2.

3.2 Numerical stability criterion

After the independent verification and sensitivity analysis, $\delta x = \delta y = 9\times10^{-3}$m is chosen as the homogeneous spatial resolution. For the time step, there are two stability criteria often used to determine its reasonableness for the scheme. One is associated with the convection process and the other with the diffusion process:

$$\delta t \le \min\left\{\frac{Cr\times\delta x}{u_{\max}}, \frac{Cr\times\delta y}{v_{\max}}, \frac{Cr\times\delta z}{w_{\max}}\right\} \tag{14}$$

$$\delta t \le \min\left\{\frac{\rho\times\delta x^2}{2\Gamma}, \frac{\rho\times\delta y^2}{2\Gamma}, \frac{\rho\times\delta z^2}{2\Gamma}\right\} \tag{15}$$

where δt is the time step, u, v and w are the velocities of x, y and z directions, respectively. C_r is the Courant number which characterizes the convection process. ρ is the density and Γ is the diffusion coefficient, which has different physical significance in different problems.

In principle, the value of C_r is in the range of 0.5 to 1. But for problems with highly non-linear characteristics such as sloshing, C_r is often small to ensure stability and accuracy. Since there is no negative diffusion in the sloshing problem, δt

can be identified as 1×10^{-3}s by equation (15) after preliminary calculations, which was also adopted after the sensitivity analysis.

Referring to the sloshing test based on a 6-dof platform of Wei et al. (2015)[15], the simulation is carried out with an amplitude of 0.03m and a frequency of 0.66Hz when the filling level is 20%. Figure 2 shows the comparison of the numerical and experimental results of the sloshing pressure. The sloshing has stepped into a relatively stable state at 119s. The pressure time history plot at 20%H has obvious double peaks, which can be seen in both numerical and experimental results. For the averaged first peak of pressure, the result of the numerical case is 3.404 kPa and that of the model test is 3.631 kPa. For the averaged second peak of pressure, the result of the numerical case is 1.171 kPa and that of the model test is 1.246 kPa. The difference between the numerical simulation and the model test is less than 7%. It shows that the sloshing phenomenon in the model tank can be accurately simulated by the numerical method in this research, and the spatial resolution and time step can accurately capture the impact effect of sloshing liquid.

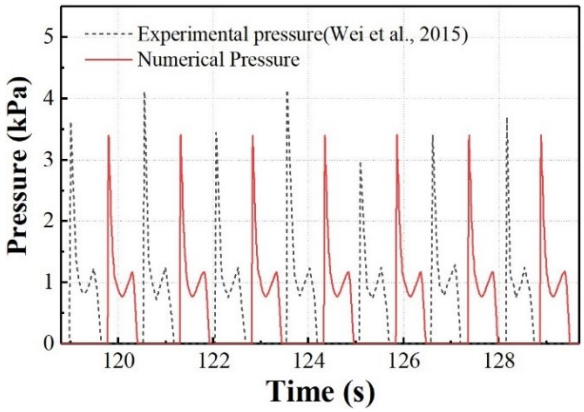

Figure 2. Comparison of the pressure history from the numerical calculation to the experimental result presented.

4. RESULTS AND DISCUSSIONS

4.1 Anti-sloshing effect of the hanging porous part

The anti-sloshing performance of the hanging porous part under medium and low filling conditions is studied in this section. The conditions are shown in Table 1 and the filling levels are 30% and 50%, respectively. The amplitude of 0.03 m is selected, which refers to the medium excitation amplitude A/B = 0.023 and the large excitation amplitude A/B = 0.047[17]. The theoretical first-order natural frequencies of the sloshing liquid in clean tank are selected as the excitation frequencies, which can be obtained by equation (15). The porosity of the parts is 50% and the midline offset is 0%H. In the following sections, the sloshing pressure at 30%H and 50%H, the wave elevation and the force on the part are analysed, and they are applied to reflect the state of the sloshing liquid and the suppression effect of the parts.

Table 1. Conditions for numerical simulations.

Cases	η (%)	f (Hz)	Suppress method
1	30	0.76	Clean
2	30	0.76	Composite method
3	50	0.85	Clean
4	50	0.85	Composite method

The time history plots of the pressure at 30%H and the wave elevation in Case 1 and Case 2 are shown in Figures 3 and 4. The hanging porous part decreases the averaged peak pressure by 77.5% and the double-peak characteristic disappears, this means the effect of impact is weakened or even disappears and the intensity of sloshing is reduced. The averaged peak value of wave elevation decreases by 79.8%, and the wave elevation turns to change symmetrically around the static free surface. It is evident that the hanging porous part can effectively suppress sloshing under low filling conditions.

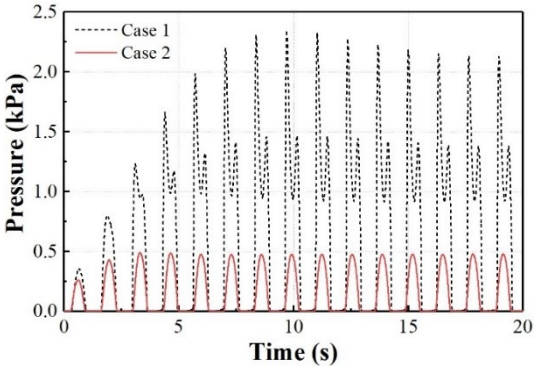

Figure 3. Pressure time history at 30%H in Case 1 and 2.

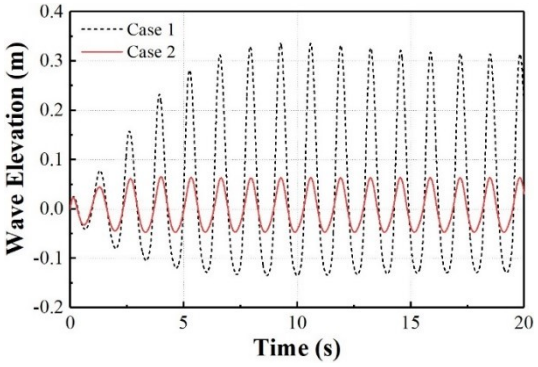

Figure 4. Wave elevation time history in Case 1 and 2.

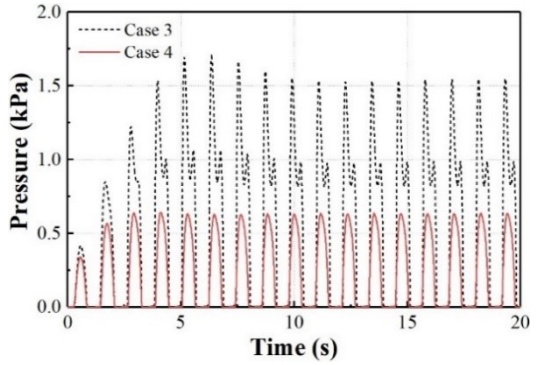

Figure 5. Pressure time history at 50%H in Case 3 and 4.

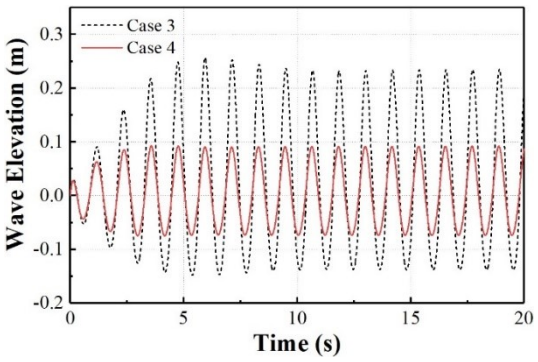

Figure 6. Wave elevation time history in Case 3 and 4.

The pressure time history at 50%H and wave elevation time history in Case 3 and 4 are shown in Figures 5 and 6. Compared with the common parts fixed at the bilge, the hanging porous parts can maintain a good anti-sloshing effect under the condition of medium filling. The hanging porous part decreases the average peak pressure by 58.8% and decreases the average peak value of wave elevation by 61.1%, which is lower than that under the 30% filling condition. Although the intensity of sloshing in the clean tank under the medium filling condition is weaker than that under the low filling condition, the peak pressure and the peak elevation under the medium filling condition become larger than that under the low filling condition in the tank with hanging porous part, which shows the damping characteristics of the hanging porous part.

4.2 Effect of porous on anti-sloshing performance

According to the Ergun formula, porosity is an important factor affecting the viscous resistance factor and inertial resistance factor of the porous part. After sloshing has stepped into a stable state, the averaged peak pressure is shown in Figure 7 and the averaged peak elevation is shown in Figure 8. The filling level of these conditions is 30% and the excitation amplitude is 0.03m. Porosity is 0% means the part is a vertical solid part.

Figures 7 and 8 show that the suppression effect of the part has the parabolic-like characteristic with the increase of the porosity, and the part can suppress sloshing more effectively when the porosity is close to 30%. According to the Ergun formula, when the porosity increases, the viscous resistance factor and inertial resistance factor decrease. This leads to a weakening of the damping effect and reduces the anti-sloshing effect of the part. It can be found from Figure 9 that the porous part changes into a solid part with the decrease of porosity, and the mass flow rate of the liquid flowing through the porous part reduces. Although the resistance factor is larger, the viscous dissipation and the inertial loss are smaller. The part mainly reduces the energy of sloshing liquid through the shear layer generated at the tips[6]. The damping effect of the part is limited by the decrease in porosity.

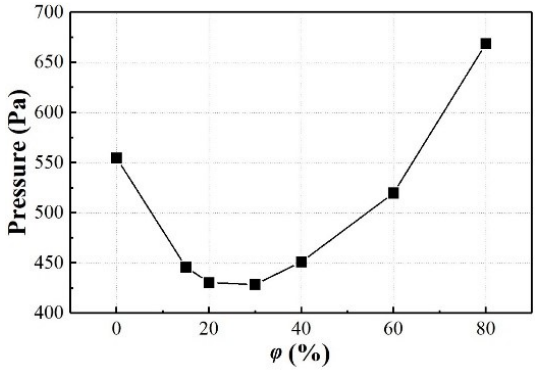

Figure 7. Maximum sloshing pressure at different porosities (η=30%, A=0.03 m).

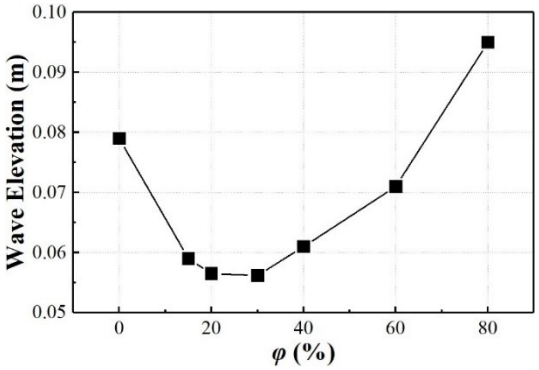

Figure 8. Maximum wave elevation at different porosities (η=30%, A=0.03 m).

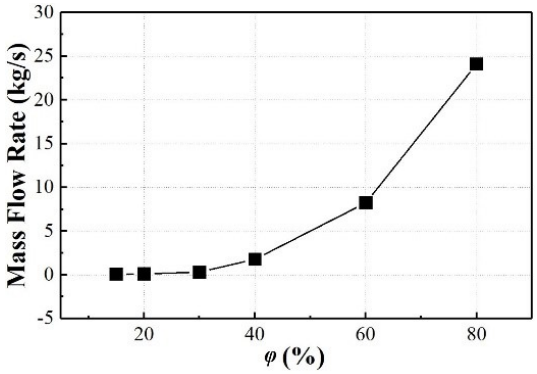

Figure 9. Mass flow rate of liquid through the porous part at different porosities (η=30%, A=0.03 m).

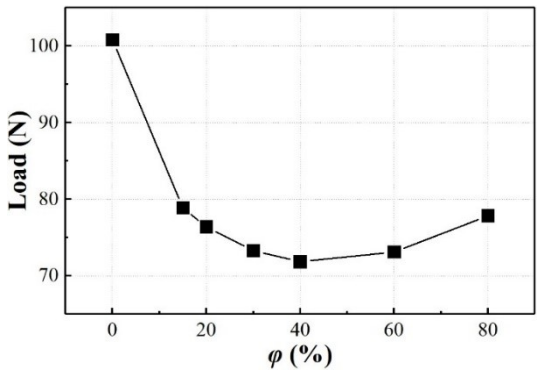

Figure 10. Maximum load acting on the part at different porosities (η=30%, A=0.03 m).

Figure 10 shows the mean peak load acting on the part. From Figures 9 and 10, it can be found that the mass flow rate of the sloshing liquid flowing through the porous part is small when porosity is lower than 30%, which leads to more sloshing liquid directly acting on the part rather than flowing through the part. At the same time, the sloshing becomes more violent due to the weakening of the anti-sloshing effect. The combined action of these factors leads to the larger load acting on part with low porosity. When the porosity is large, the damping effect is weak and the sloshing is violent. Although there is less sloshing liquid directly acting on the part, the kinetic energy of sloshing liquid increases, which causes the load acting on the part not to keep decreasing as the porosity increases. As an important factor affecting the damping effect, porosity has a direct effect on the suppression effect and the safety of the hanging porous part. In order to ensure better overall performance of the hanging porous part, the appropriate porosity should make the part have a larger resistance factor and keep the appropriate mass flow rate of the liquid flowing through the part.

4.3 Effect of midline offset on anti-sloshing performance

The midline offset is also an important structural parameter of the hanging porous part, which determines the mass flow rate of the liquid affected by the damping effect and the mass flow rate of the liquid flowing through the part. Under the conditions of 30% filling, the medium excitation A=0.03 m and the large excitation A=0.05 m are applied to investigate the effect of midline offset on suppression performance in sloshing with different intensities. Figures 11 and 12 show the variation of the averaged peak pressure and the averaged peak elevation under the conditions of different excitation amplitudes.

When the midline of the hanging porous part is offset downward relative to the static free surface, $\lambda < 0$, the averaged peak pressure and the averaged peak elevation decrease, which means the sloshing is further suppressed. At the same time, the

averaged peak value of the pressure and the wave elevation under the large excitation condition approaches that under the medium excitation condition, which means that the damping effect of the part becomes stronger. When the negative offset increases, the contact area between the part and the high-velocity sloshing liquid near the free surface increases.

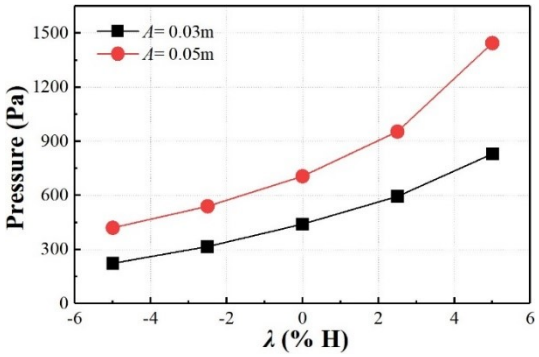

Figure 11. Variation of maximum sloshing pressure with midline offset (η=30%, φ=30%).

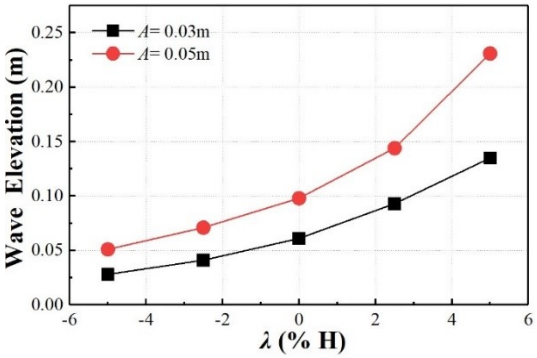

Figure 12. Variation of wave elevation with midline offset (η=30%, φ=30%).

Figure 13 shows the sloshing state with a midline offset of ±2.5%H under the conditions of different excitation amplitudes, and the dotted line means the static free surface. The time of the sloshing state in Figure 13 is the time when the sloshing liquid reaches the maximum velocity before impacting the wall in the 8th sloshing period. More high-velocity liquid flows through the part when the midline is offset downward, which leads to a decrease in the velocity of the liquid reaching the lower tips of the part, and the liquid moving downward along the part enters a deeper low-velocity region. Therefore, the downward offset of the midline not only enhances the damping effect of the hanging porous part but also enhances the viscous dissipation in the sloshing liquid. It can be found that the hanging porous part has better anti-sloshing performance with the decrease of the midline offset.

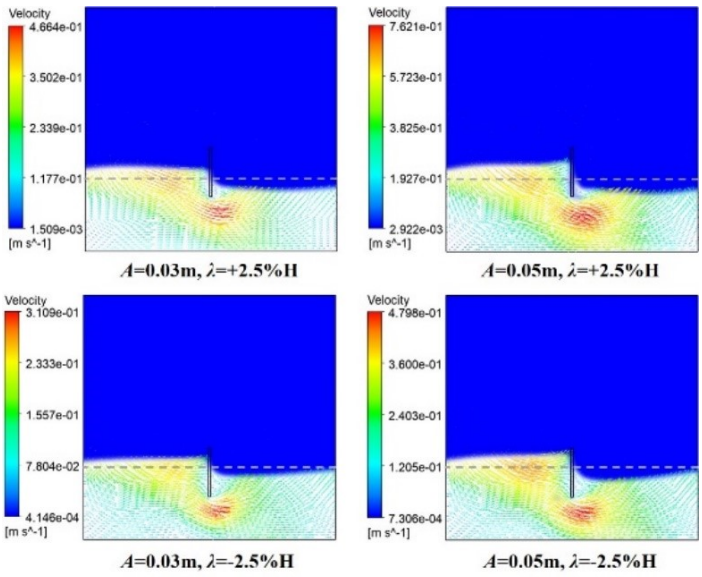

Figure 13. Sloshing states in the tank at different excitations and offsets (η=30%, φ =30%).

Although the downward offset of the midline increases the possibility of liquid climbing over the part, the stronger damping effect reduces the kinetic energy of the sloshing liquid, there is little high-velocity liquid climbing over the part and directing impacting the wall. As shown in Figure 14, the peak pressure in the sloshing period occurred at 9.7s. The sloshing liquid does not climb over the part before impacting the wall. Part of the liquid flow through the porous part during the

sloshing liquid climbing along the part, which also limits the ability of the liquid to climb along the part. It also can be seen that the hanging porous part has strong adaptability to the changes in sloshing conditions. As shown in Figure 15, the more sloshing liquid acts on the part when the midline of the hanging porous part is offset downward, which causes an increase in the load acting on the part. In view of the risks of structural failure associated with the enhancement of the anti-sloshing effect, the offset of the midline needs to be carefully considered in the design process.

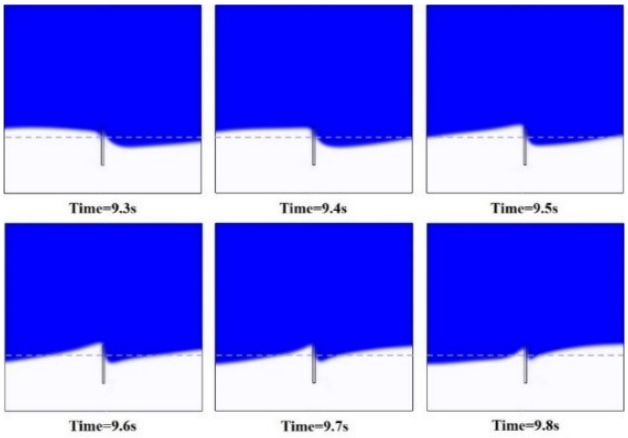

Figure 14. Free surface contour for sloshing liquid at λ= -5%H (η=30%, A=0.05 m, φ =30%).

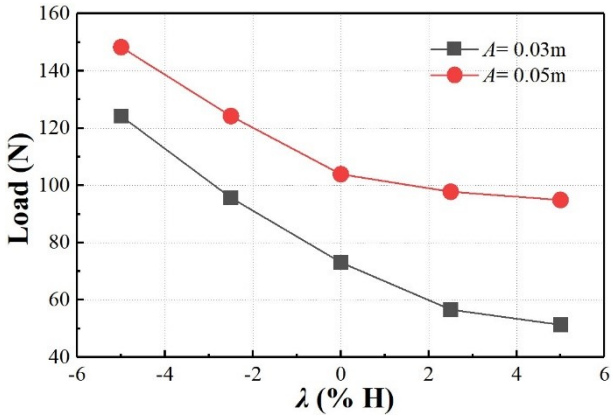

Figure 15. Maximum load acting on the part at different midline offsets (η=30%, φ =30%).

5. CONCLUSION

Through discussions of the sloshing pressure, the wave elevation and the force acting on the part, the anti-sloshing performance of the hanging porous part is numerically studied in this research. The results show that the hanging porous part with appropriate porosity and midline offset can effectively suppress sloshing under low and medium filling conditions. The main conclusions are as follows:

(1) The hanging porous part can effectively suppress the sloshing. Due to the damping characteristic, the anti-sloshing effect of the part increases with the increase of the sloshing intensity.

(2) Compared with the solid part, the hanging porous part with the appropriate porosity can not only suppress the sloshing more effectively but is also subject to weaker impact.

(3) The resistance factor is too small with the large porosity, which weakens the anti-sloshing effect. Too small porosity reduces the mass flow rate of the liquid flowing through the part, this limits the anti-sloshing performance of the part. Although the mass flow rate of the liquid directly acting on the part is small when the porosity is large, the more violent sloshing still increases the load acting on the part.

(4) When the midline of the hanging porous part is offset downward, the damping effect of the part increase, which increase the anti-sloshing of the part. Due to the damping effect, the hanging porous part has strong adaptability to the changes in sloshing conditions. The sloshing liquid does not climb over the part easily, so the anti-sloshing effect of this method does not weaken easily. The downward offset of the midline causes the increase of the load acting on the part.

ACKNOWLEDGEMENT

The work presented in this paper has been carried out under the co-support provided by the Postgraduate Research & Practice Innovation Program of Jiangsu Province (Grant No. SJCX21_1486), and the Open fund project of Jiangsu Institute of Marine Resources Development (Grant No. JSIMR202009). The authors would like to acknowledge the co-support.

REFERENCES

[1] Park, J., Kim S. and Kim Y., "Study on tank shape for sloshing assessment of LNG vessels under unrestricted filling operation," Journal of Marine Science and Technology, 20, 640-651(2015).
[2] Faltinsen, O. M., Rognebakke, O. F. and Timokha, A. N., "Transient and steady-state amplitudes of resonant three-dimensional sloshing in a square base tank with a finite fluid depth," Phys. Fluids, 18(1), 012103(2006).
[3] Hara, F. and Shibata, H., "Experimental study on active suppression by gas bubble injection for earthquake induced sloshing in tanks," JSME International Journal, 30(260), 318-323(1987).
[4] Zou, C. F., Wang, D. Y. and Cai, Z. H., "Effect of boundary layer and liquid viscosity and compressible air on sloshing characteristics," International Journal of Naval Architecture and Ocean Engineering, 7(4), 670-690(2015).
[5] Hernandez, E. and Santamarina, D., "Active control of sloshing in containers with elastic baffle plates," International Journal for Numerical Methods in Engineering, 91(6), 604-621(2012).
[6] Shao, J., Li, S., Li, Z., et al., "A comparative study of different battles on mitigating liquid sloshing in a rectangular tank due to a horizontal excitation," Engineering Computation, 32(4), 1172-1190(2015).
[7] Zou, C. F., Wang, D. Y., Cai, Z. H., et al., "The effect of liquid viscosity on sloshing characteristics," Journal of Marine Science and Technology, 20(4), 765-775(2015).
[8] Ünal, U. O., Bilici, G., Akyıldız, H., "Liquid sloshing in a two-dimensional rectangular tank: A numerical investigation with a T-shaped baffle," Ocean Engineering, 187, 106183 (2019).
[9] Koh, C. G., Luo, M., Gao, M., et al., "Modelling of liquid sloshing with constrained floating baffle," Computers and Structures, 122, 270-279(2013).
[10] Yu, Y., Ma, N., Fan, S., et al., "Experimental and numerical studies on sloshing in a membrane-type LNG tank with two floating plates," Ocean Engineering, 129, 217-227(2017).
[11] Zang, Q., Liu, J., Yu, J., et al., "Boundary element analysis of liquid sloshing characteristics in axisymmetric tanks with various porous baffles," Applied Ocean Research, 93, 101963(2019).
[12] Xue, M., Jiang, Z., Hu, Y., et al., "Numerical study of porous material layer effects on mitigating sloshing in a membrane LNG tank," Ocean Engineering, 218, 108240(2020).
[13] MacDonald, I. F., El-Sayed, M. S., Mow, K., et al., "Flow through porous media-the Ergun equation revised," Ind. Eng. Chem. Fund, 18(3), 199-208(1979).
[14] Wu, C., Faltinsen, O. and Chen, B., "Numerical study of sloshing liquid in tanks with baffles by time-independent finite difference and fictitious cell method," Computers & Fluids. 63, 9-26(2012).
[15] Wei, Z. J., Chen, X. D., Dong, Y. S., et al. "An experimental study of slamming impact load on two platforms," Journal of Ship Mechanics, 19(7), 841-849(2015).
[16] Liu, D. M. and Lin, P. Z., "A numerical study of three-dimensional liquid sloshing in tanks," Journal of Computational Physics, 227(8), 3921-3939(2008).
[17] Gurusamy, S., Sanapala, V. S., Kumar, D., et al., "Sloshing dynamics of shallow water tanks: Modal characteristics of hydraulic jumps," Journal of Fluids and Structures, 104, 103322 (2021).